Cécile Raillard*, Valérie Héquet, Bifen Gao, Heyok Choi, Dionysios D. Dionysiou, Arnaud Marvilliers, and Bertrand Illien

Correlations between Molecular Descriptors from Various Volatile Organic Compounds and Photocatalytic Oxidation Kinetic Constants

Abstract: The photocatalytic oxidation of seven typical indoor volatile organic compounds (VOCs) is experimentally investigated using novel nanocrystalline TiO_2 dip-coated catalysts. Not only the role of hydrophilicity of the reactants but also other physico-chemical properties and molecular descriptors are studied and related to kinetic and equilibrium constants. The main objective of this work consists in establishing simple relationships that will be useful to deepen the understanding of gas-phase heterogeneous photocatalytic mechanisms and for the prediction of degradation rates of these VOCs using an indoor air treatment process.

Keywords: photocatalytic oxidation, molecular modeling, quantitative structure–activity relation (QSAR)

***Corresponding author: Cécile Raillard**, L'UNAM, GEPEA, UMR CNRS 6144, Nantes cedex 03, France,
E-mail: Cecile.Raillard@univ-nantes.fr
Valérie Héquet, L'UNAM, GEPEA, UMR CNRS 6144, Ecole des Mines de Nantes, Nantes cedex 03, France,
E-mail: Valerie.Hequet@mines-nantes.fr
Bifen Gao, L'UNAM, GEPEA, UMR CNRS 6144, Ecole des Mines de Nantes, Nantes cedex 03, France, E-mail: BFGAO@ntu.edu.sg
Heyok Choi, Department of Civil engineering, University of Texas at Arlington, Arlington, TX 76019, USA, E-mail: hchoi@uta.edu
Dionysios D. Dionysiou, University of Cincinnati, Cincinnati, OH 45221, USA, E-mail: dionysdd@ucmail.uc.edu
Arnaud Marvilliers, LCSNSA, EA2212, UFR Sciences Technologies, Université de la Réunion, Saint-Denis 97715, Réunion,
E-mail: Arnaud.Marvilliers@univ-reunion.fr
Bertrand Illien, LCSNSA, EA2212, UFR Sciences Technologies, Université de la Réunion, Saint-Denis 97715, Réunion,
E-mail: bertrand.illien@univ-reunion.fr

1 Introduction

Today, the risks associated with poor indoor air quality (IAQ) at home and in the workplace are being increasingly acknowledged [1]. Some studies have shown that in modern industrial countries, such as the United States and Germany, people can spend 15–16 h a day at their home and domestic environments, depending on how they spend their work and leisure time [2]. Susceptible individuals are, therefore, at a far greater risk of adverse health effects as a result of being subjected to chronic low levels exposure to indoor air pollutants over time. Along with particulate matter and microbial contaminants, volatile organic compounds (VOCs) represent the main common type of air pollutants encountered indoors. Therefore, there is a growing interest in developing processes applicable to indoor air purification aimed at destroying these compounds [3]. Among numerous possible treatments, gas-phase photocatalytic oxidation (PCO) using TiO_2 as photocatalyst appears to be a very promising, convenient and innovative technology for the improvement of IAQ [4]. Numerous parameters influence the efficiency of the process: humidity, pollutant chemical group, type of TiO_2 etc. Specific studies focusing on the photochemical degradation of VOCs noted a strong but contrasting influence of water vapor depending on the considered pollutant [5]. The influence of TiO_2 coating type (powder and sol–gel film) over the role of water vapor on the PCO of a typical indoor air pollutant has also been regarded [6]. A layer of physisorbed water was thought to be formed at the catalyst surface for TiO_2 films when the relative humidity was high enough attributed to their hydrophilic and even superhydrophilic properties [7–12]. A subsequent work was conducted dealing with the influence of aqueous solubility of various VOCs on their photocatalytic degradation using such TiO_2 film photocatalysts. Regarding the obtained results, it was concluded that a higher aqueous solubility seems to have a negative influence on the photocatalytic degradation using TiO_2 films. However, this trend has to be confirmed by performing further experiments with other VOCs in a large range of hydrophilicities [13]. Furthermore, the roles of other parameters describing some physical and chemical properties of the reactants also have to be examined. As it is impossible to study

every pollutant present in indoor air, most abundant molecules must be considered for such work. The studied molecules can then be grouped by family in order to attempt to find preponderant photocatalytic mechanisms by a family of molecules. To do so, a quantitative structure–activity relationship (QSAR) can be implemented. QSAR studies concern a very large domain of applications among which photocatalysis is included [14–19]. Most studies have been performed in aqueous phase using P25 TiO_2 in suspension. Furthermore, except for the study carried out by Yu et al. [14], the PCO rate has often been predicted by the apparent first-order kinetic constant, the initial reaction rate or the half-life time. However, the assumption that the PCO reaction is a first-order reaction is not always relevant [14].

Therefore, the aim of the current work is to assess the role of hydrophilicity and other molecular descriptors on adsorption and PCO of gaseous pollutants using films of TiO_2. Adsorption isotherms were carried out and modeled for the calculations of adsorption constants. Then, based on the methodology described by Fogler [20] for heterogeneous catalytic reactions, the reaction mechanism was approached and a kinetic rate law was expressed. Kinetic and adsorption constants were deduced from the experimental results and related to physico-chemical parameters. The main objective of this study is to establish simple relationships that will be useful for understanding gas-phase heterogeneous photocatalytic mechanisms and, later, for predicting degradation rates of these VOCs using an indoor air treatment.

2 Material and methods

2.1 TiO_2 photocatalysts

Mesoporous TiO_2-anatase films synthesized by sol–gel route and dip-coated on borosilicate glass substrates are used [21]. The main characteristics of the photocatalyst are summarized in Table 1.

Table 1 Photocatalyst characteristics.

Coating dimensions	BET surface area	Pore volume	Pore diameter	TiO_2 crystalline phase
26 mm × 76 mm (19.8 cm²)	147 $m^2\ g^{-1}$	0.221 $cm^3\ g^{-1}$	2–8 nm	Anatase

2.2 Tested VOCs

Seven VOCs were chosen as typical indoor air pollutants among families of pollutants that are very frequently detected in indoor atmospheres. The target families were alcohols, alkanes, aldehydes and ketones. As the objective of the study was to be able to make predictions for groups of molecules, the chosen molecules were separated into two groups. One group was constituted of five molecules containing four atoms of carbon: methyl ethyl ketone (MEK), butyraldehyde, 1-butanol, n-butane and iso-butane. With this first group, the common parameter is the number of atoms of carbon but the influence of the chemical function can be assessed. The other group contains four alkanes: *n*-butane, iso-butane, pentane and hexane. With this second group, only alkanes are represented, enabling the influence of the number of atoms of carbon to be established. The organics were purchased from Aldrich Chemicals and used directly as received. The VOCs concentrations in the gas phase were followed by gas chromatography and a flame ionization detector.

2.3 Adsorption isotherms (gas–solid interface)

Adsorption isotherms were carried out in 2L-batch reactors in the dark. The temperature was controlled and fixed at 30°C. The relative humidity was set at 30% for this temperature. Five different concentrations ranging from 2 to 100 mmol m^{-3} were implemented for each VOC. Each isotherm was repeated twice to ensure the reproducibility of the results. Once the equilibrium was reached, the concentration C_e in the gas phase was measured. Then, the quantity of adsorbed pollutant was calculated for each initial concentration C_0 by the following relation:

$$q_e = \frac{(C_0 - C_e)V}{S} \quad [1]$$

where V is the reactor volume (m^3) and S is the catalyst surface (m^2).

Finally, adsorption isotherm curves, representing the adsorbed quantity of pollutant by surface unit of material at the equilibrium (q_e, mmol $m^{-2}_{catalyst}$) as a function of the pollutant concentration in the gas phase at the equilibrium (C_e, mmol m^{-3}), were plotted and modelled in order to calculate adsorption constants.

2.4 Photocatalytic reactor

The gas-phase photocatalytic oxidation of the VOCs was studied at a fixed temperature of 30°C in a batch reactor equipped with a medium pressure mercury lamp (Heraeus TQ 718 Z4, 700 W, $\lambda_{max} = 365$ nm, $I = 3$ mW cm^{-2}). The relative humidity was fixed at 30% at 30°C ± 1°C. More details on the experimental procedure are given elsewhere [6, 22].

2.5 Rate law establishment

VOCs were tested at different initial concentrations ranging from 10 to 50 mmol m^{-3}. A rate law consistent with experimental observation and based on a simplified mechanism can be written for the photocatalytic degradation of VOCs in the used batch reactor. The hypotheses taken into account to write the mechanism are listed below.

1) In the range of studied concentrations, it is assumed that adsorption is a Langmuirian-type adsorption as shown in the previous paper [23].
2) Oxygen is in excess in comparison to other reactants.
3) Adsorption of carbon dioxide onto the photocatalyst is neglected [24].
4) Adsorption of water vapor on the photocatalytic media is not taken into account. Competitive adsorption between water vapor and studied solutes as well as possible dissolution of studied molecules in a film of water at the catalyst surface does not appear directly in the reaction rate.
5) Surface reaction is rate-controlling [20].
6) Reaction is carried out at steady state.
7) Only adsorbed species are involved in the chemical transformation.
8) For VOCs initial concentrations lower than 50 mmol m^{-3}, reaction intermediates are neglected.

Eqs. (2–4) below represent the proposed mechanism for this reaction.

$$R + S \rightleftharpoons R.S \quad \text{adsorption of VOC on the surface} \qquad [2]$$

$$R.S \rightarrow P.S \quad \text{surface reaction to form products} \qquad [3]$$

$$P.S \rightleftharpoons P + S \quad \text{desorption of products from the surface} \qquad [4]$$

Then each step is treated as an elementary reaction for writing the rate laws. The rate expression r_{AD} for the adsorption of VOC as given in eq. [2] is

$$r_{AD} = k_A\left(C_R C_v - \frac{C_{R.S}}{K_A}\right) \qquad [5]$$

where C_R is the VOC concentration in the gas phase, C_v is the number of moles of vacant sites per unit mass of catalyst, $C_{R\cdot S}$ is the surface concentration of sites occupied by R, k_A is the kinetic constant for the attachment process and K_A is the adsorption equilibrium constant.

The rate law for the surface reaction step which is irreversible here is

$$r_S = k_S C_{R.S} \qquad [6]$$

where k_S is the surface reaction rate constant.

The rate for products desorption is

$$r_D = k_D(C_{P.S} - K_D C_P C_v) \qquad [7]$$

where k_D is the desorption rate constant, $C_{P.S}$ is the surface concentration of sites occupied by P, C_P is the concentration of P in the gaseous phase and K_D is the adsorption equilibrium constant of P.

As surface reaction is rate-limiting, the global reaction rate law is equal to the surface reaction rate law ($r_R = r_S = k_S C_{R.S}$). Since the concentrations of adsorbed species cannot be readily measured, adsorption and desorption steps are used to express $C_{R.S}$ versus measurable variables. Since the reaction is carried out at steady-state conditions and surface reaction is rate-controlling, it becomes

$$\frac{r_{AD}}{k_A} = \frac{r_D}{k_D} \approx 0$$

Consequently, a relationship for the surface concentration of adsorbed VOC can be obtained:

$$C_{R.S} = K_A C_R C_v \qquad [8]$$

At this stage, the only variable left to eliminate is C_v. Since the total concentration of sites is

$$C_t = C_v + C_{R.S} + C_{P.S} = C_v(1 + K_A C_R + K_D C_P) \qquad [9]$$

and the formed intermediates and by-products (P) are neglected in this study, the global reaction rate law is written as

$$r_R = \frac{k_g K_A C_R}{1 + K_A C_R} \qquad [10]$$

where $k_g = k_s C_t$ is the global reaction rate constant.

This relation is also valid at the initial time of the reaction so that, knowing only the initial concentration

and the initial reaction rate, the constants k_g and K_A can be determined.

For each operating condition, a kinetic curve was drawn and used to determine the initial reaction rate (r_0). Numerous approaches are possible to calculate the initial degradation rate. In the present work, degradation kinetics ($C = f(t)$) were fitted by a third-order polynomial. The initial reaction rate was thus equal to the derivative of this polynomial at the initial time ($r_0 = -(dC/dt)_{t=0}$).

2.6 Descriptors calculations and significations

The chosen molecular descriptors are parameters that encode quantitative information about molecular structure and include both data obtained experimentally, and parameters derived from quantum chemical calculations. The Gaussian package [25] has been used for all quantum chemical calculations. Geometry optimizations of each compound in its fundamental state ($E°$) was first performed at the B3LYP/6–31+G** density functional level. Then descriptors calculations were done with these optimized geometries with the same method if not otherwise stated. The aim was to obtain three categories of molecular descriptors. The first group may be related to the van der Waals interactions and the physical adsorption phenomenon. The descriptors are the molecular volume (MV), the dipole moment (μ), two invariants of the electric static polarizability tensor, the mean polarizability ($\overline{\alpha}$) and the polarizability anisotropy ($\Delta\alpha$) [26]. The second group may correspond to the electronic stability reflecting the reactivity of the molecule, the descriptors are the highest occupied molecular orbital (HOMO) and lowest unoccupied molecular orbital (LUMO) energies (respectively, E_{HOMO} and E_{LUMO}) and hardness ($\eta = (E_{LUMO} - E_{HOMO})/2$) [27]. Hardness is a measure of the resistance of a chemical species to change its electronic configuration. The third group may primarily represent the affinity of the molecules with water vapor and hydrophilic surfaces, enabling absorption or dissolution phenomena to be described; they are the molecular electrostatic potential ($V_{s,min}$) and the solvation free energy in water (ΔG_{solv}).

Some physico-chemical parameters were also considered and found in the literature: solubility S, partition coefficient octanol–water K_{ow}, Henry's constant $K°_H$ and VOCs-hydroxyl radical rate constant k_{OH}. These parameters are used to establish a preliminary relation between the kinetic and adsorption constants that were obtained in the experimental part. The strategy is to put the kinetic constant into relation with descriptors that are susceptible to better described reactivity, and to put the equilibrium constant into relation with descriptors susceptible to better describe the adsorption or absorption phenomena that can occur during the photocatalytic degradation of the target molecules. The second stage is then to relate the physico-chemical parameters to calculated molecular descriptors and to finally establish a link between experimental data and the molecular descriptors.

The volume of a molecule (MV) is defined by the volume occupied by the 0.001 au electron density envelope [28]. This value is generally considered to provide a reasonable definition of the "molecular shape" volume (i.e. free from lost area due to the packing in the liquid). The electric static polarizability tensor components are calculated at MP2(full)/6–311++G(3df,2pd) level. Then $\overline{\alpha}$ and $\Delta\alpha$ are calculated according to $\bar{\alpha} = \frac{1}{3}(\alpha_{xx} + \alpha_{yy} + \alpha_{zz})$

$$(\Delta\alpha)^2 = \frac{1}{2}\Big[(\alpha_{xx} - \alpha_{yy})^2 + (\alpha_{xx} - \alpha_{zz})^2 + (\alpha_{yy} - \alpha_{zz})^2 + 6\left(\alpha_{xy}^2 + \alpha_{yz}^2 + \alpha_{xz}^2\right)\Big]$$

where x, y and z are the principal axes of the molecule.

HOMO, LUMO and hardness energies are calculated at the HF/6–31+G** level because Hartree-Fock method follows the Koopmans' theorem [29]. $V_{s,min}$ is the minimum electrostatic potential on the 0.001 au electron density envelope. Potential electrostatic minima on the molecular surface symbolize the site of electron localization on the molecular surface, indicating the sites for electrophilic attack or hydrogen bond formation. The solvation free energy in water (ΔG_{solv}) is calculated using the polarizable continuum model using the integral equation formalism variant (IEF-PCM) with the UAKS radii parameter set as implemented in Gaussian software.

Table 2, below, sets out the results of the calculations for the chosen molecular descriptors as well as some physico-chemical parameters found in the literature.

3 Results and discussion

3.1 Adsorption isotherms

The methodology described above was applied twice for the seven VOCs studied. Figure 1 displays the results corresponding to all experimental points for *n*-butane and MEK. Regarding Figure 1, it can be observed that the isotherm curves exhibit a two-step-like behavior

Table 2 Calculated molecular descriptors and other physico-chemical parameters.

Parameter	*n*-Butane	Iso-butane	Pentane	Hexane	1-Butanol	MEK	Butyraldehyde
E^o (au)	−158.47659	−158.47753	−197.79395	−237.11129	−233.69237	−232.49223	−232.48045
μ (Debye)	0	0.13	0.08	0	1.73	3.04	2.82
Molecular volume MV (cm^3/mol)	68.3	68.5	82.8	97.7	75.1	69.9	69.4
E_{HOMO} (au)	−0.45670	−0.45709	−0.44821	−0.44022	−0.44129	−0.41132	−0.42089
E_{LUMO} (au)	0.08709	0.08480	0.08753	0.08411	0.07225	0.07327	0.07859
Electrostatic potential $V_{s,min}$ (kcal/mol)	−2.33	−2.21	−2.43	−2.43	−36.28	−37.58	−35.41
Solvation free energy ΔG_{solv} (kcal/mol)	2.09	2.34	2.26	2.43	−5.00	−4.39	−3.53
Mean polarizability $\bar{\alpha}$ (10^{-24} cm^3)	7.77	7.77	9.59	11.43	8.43	7.88	7.91
Polarizability anisotropy $\Delta\alpha$ (10^{-24} cm^3)	1.82	1.02	2.62	3.65	2.31	2.31	2.40
Hardness η (au)	0.27189	0.27094	0.26787	0.26216	0.25677	0.24229	0.24974
log K_{ow}	2.89	2.76	3.45	3.9	0.88	0.29	0.88
Solubility at 25°C S (g L^{-1})*	0.0614	0.054	0.038	0.0095	74	211.4	66.3
k_{OH}** (cm^3 $molecule^{-1}$ s^{-1})	$2.54.10^{-12}$	$2.34.10^{-12}$	$3.94.10^{-12}$	$5.61.10^{-12}$	$8.30.10^{-12}$	$1.15.10^{-12}$	$2.35.10^{-11}$
K^o_H*** (mol/kg bar)	0.0011	0.00086	0.00078	0.00155	191.6	25.7	13.95

Notes: au: atomic unit, *Yalkowski and He [30], **Atkinson [31], ***Staudinger and Roberts [32] (hexane, 1-butanol, butyraldehyde, MEK); Yaws and Yang [33] (*n*-butane, isobutane, pentane).

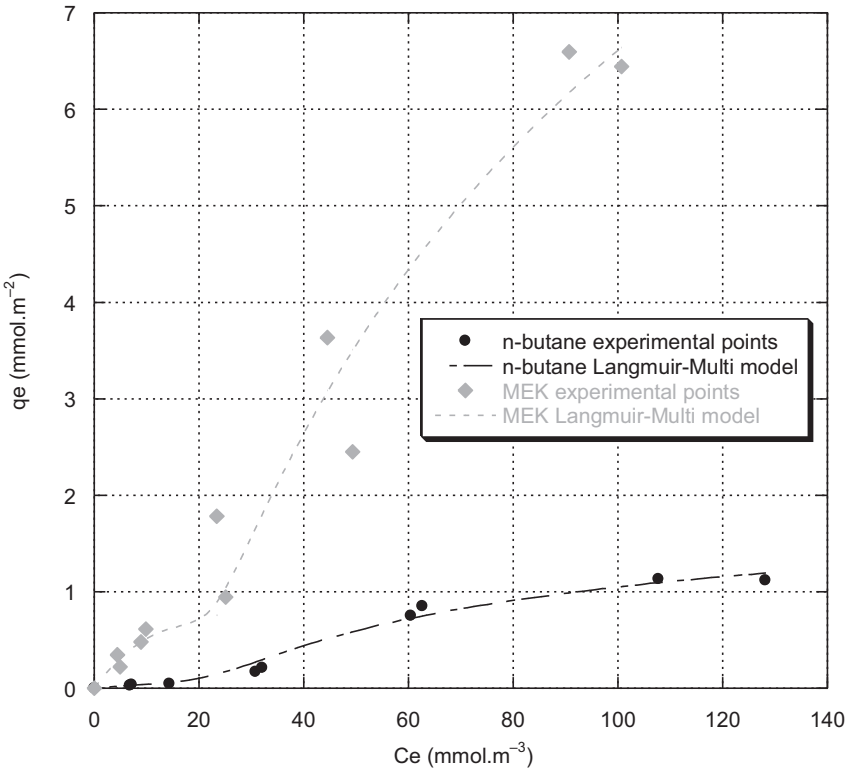

Figure 1 Examples of adsorption isotherm curves and fitting of the "Langmuir-multi" model to the experimental results.

with an inflexion point around a concentration in the gas phase C_{inf} around 25 mmol m^{-3}.

In a previous paper, a specific model, called "Langmuir-multi" was built to fit adsorption experimental data presenting the same shape [23]. In this model, it is considered that the first part of the curve corresponds to a Langmuirian-type adsorption and that several mechanisms are involved in the second part of the curve, such as the presence of heterogeneous sites, multilayer adsorption and other possible occurring phenomena. According to these hypotheses, the Langmuir equation is kept in the first part of the curve (eq. [11]) and for higher C_e, the Langmuir–Freundlich equation is applied, taking the different possible mechanisms into account overall (eq. [12]):

Table 3 "Langmuir-multi" constants for the seven tested molecules.

	q_{m1} (mmol m^{-2})	b_1 (m^3 mmol^{-1})	q_{m2} (mmol m^{-2})	b_2 (m^3 mmol^{-1})	r
***n*-Butane**	**0.11** ± 0.04	0.06 ± 0.03	1.9 ± 0.4	0.015 ± 0.006	0.992
Pentane	**0.17** ± 0.14	0.10 ± 0.15	3.5 ± 1.8	0.007 ± 0.005	0.990
Hexane	**0.17** ± 0.04	0.18 ± 0.09	1.2 ± 1.0	0.016 ± 0.024	0.954
Iso-butane	**0.18** ± 0.10	0.06 ± 0.05	3.7 ± 2.0	0.004 ± 0.003	0.992
Butyraldehyde	**0.41** ± 0.07	0.61 ± 0.55	14.4 ± 5.8	0.019 ± 0.017	0.938
MEK	**1.85** ± 0.45	0.04 ± 0.02	14.6 ± 7.5	0.010 ± 0.009	0.977
1-Butanol	**2.51** ± 0.45	0.09 ± 0.03	13.1 ± 5.3	0.021 ± 0.018	0.961

The equation of this new model is given below:

$$\text{For } 0 \le C_e \le C_{inf},\ q_e = \frac{q_{m1} b_1 C_e}{1 + b_1 C_e} \quad [11]$$

$$\text{For } C_e \ge C_{inf},\ q_e = q_{m1}\frac{b_1 C_e}{1 + b_1 C_e} + q_{m2}\frac{b_2 (C_e - C_{inf})^n}{1 + b_2 (C_e - C_{inf})^n} \quad [12]$$

where b_1 and b_2 are the adsorption constants (m^3 mmol^{-1} and m^{3n} mmol^{-n}, respectively), and q_{m1} and q_{m2} are the maximum adsorption capacities (mmol m^{-2}). In the present work, n was taken equal to 1. The "Langmuir-multi" constants for the seven compounds are listed in Table 3.

From the results displayed in Table 3, it can be observed that the "Langmuir-multi" model fits the experimental data correctly. The correlation coefficients are satisfying, and comprised between 0.954 and 0.992. However, the uncertainty on the calculated constants is quite high, particularly for b_1 and b_2. The uncertainty on b_1 and b_2 constants comes from the low number of experimental points obtained for equilibrium concentrations under 15 mmol m^{-3}. Consequently, further work will focus only on q_{m1} and q_{m2} constants. We also remark that alkanes are not well-adsorbed on TiO_2. Considering only the first part of the isotherm curves and the value of q_{m1}, the adsorption of VOCs onto TiO_2 can be classified as follows: 1-butanol > MEK > butyraldehyde > iso-butane = hexane = pentane = *n*-butane. Looking at the adsorption behavior, the studied molecules can be divided into two groups: alkanes that are not well-adsorbed and the three other compounds belonging to the families of alcohols, ketones and aldehydes. This is in accordance with results found in the literature [34].

The following stage, presented below, is then able to establish relations between q_{m1}, q_{m2} and the chosen molecular descriptors. Proceeding in this way, it will be possible to approach the influencing factors on q_{m1} and q_{m2} values considering physical adsorption but also the possible adsorption competition with water as well as chemical sorption and/or dissolution into water cluster.

Relations between adsorption capacities (q_{m1}, q_{m2}) and molecular descriptors

In the first step, correlations between adsorption parameters derived from the "Langmuir-multi" model and the calculated molecular descriptors were sought. For the whole set of tested VOCs, the better correlation was obtained between the maximum adsorption capacity on the first part of the isotherm curve q_{m1} and the LUMO energy (Figure 2).

It was found that the q_{m1} parameter decreases exponentially when E_{LUMO} increases. The correlation coefficient reached 0.991. Contrary to what we expected, this result might indicate that chemical sorption occurs between the photocatalyst and the VOCs instead of physical adsorption governed by London forces. Chemical sorption on TiO_2 has already been proved on TiO_2 films deposited on silicon wafer (Si-TiO_2) under air atmosphere by Joung et al. [35]. As related by other authors [36] when E_{LUMO} or the gap between E_{HOMO} and E_{LUMO} is higher the molecule is less reactive. Then molecules with a higher E_{LUMO} may be less easily chemically adsorbed on TiO_2 surface.

By considering two groups in the tested VOCs, linear relationships can be obtained between q_{m1} and the solvation free energy (Figure 3). For the group containing 1-butanol, MEK and butyraldehyde, the correlation coefficient is quite high (0.993) for the linear relationship between q_{m1} and ΔG_{solv}. For the alkanes group, the correlation coefficient is lower (0.867) certainly because (a) the ΔG_{solv} values are very close for these compounds, (b) pentane and isobutane have large uncertainties on q_{m1} values.

In the presence of humidity, the surface of titania is hydroxylated due to its extreme hydrophilicity. Almost all the surface adsorption sites of TiO_2 are occupied by water molecules and hydroxyl groups are formed. By forming the OH...p electron-type interaction, VOCs could also be adsorbed on the same hydroxyl groups [37]. It is very

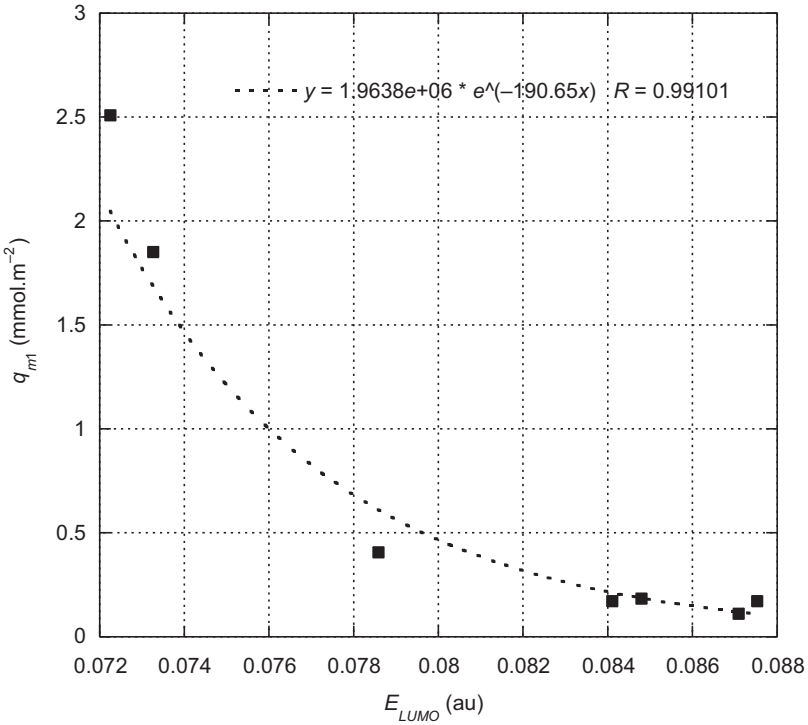

Figure 2 Relationship between q_{m1} and E_{LUMO}.

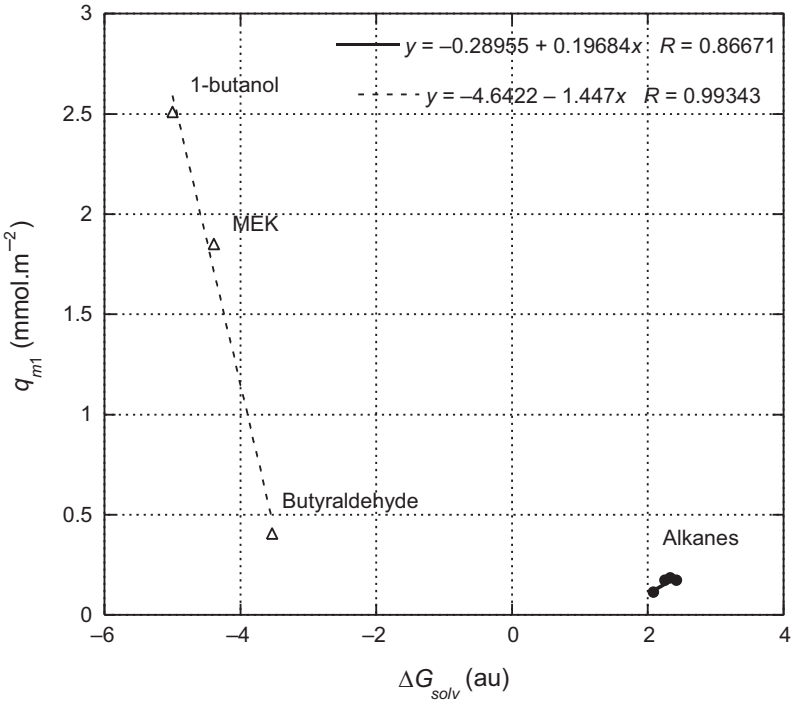

Figure 3 Relationships between q_{m1} and ΔG_{solv}.

difficult for hydrophobic organic compounds to be adsorbed on the surface of TiO_2 in the presence of water [14]. Butyraldehyde and MEK are hydrogen bond acceptors (HBA), thanks to their sp^2 hybridized oxygen atom. Both compounds can be hydrogen bonded to hydrogen atom of water or hydroxyl molecules which are already adsorbed on TiO_2 surface. MEK is a better HBA than butyraldehyde as showed by its biggest $V_{s,min}$. It may be the reason why MEK has a higher q_{m1} value than butyraldhehyde. The case of 1-butanol is different as it is

Table 4 Best relationships between q_{m2} and molecular descriptors.

Molecular descriptor	Relationship	Correlation coefficient
Partition coefficient octanol–water K_{ow}	$q_{m_2} = 16.474 - 4.1829 \log K_{ow}$	R = 0.96970
Solvation free energy ΔG_{solv}	$q_{m_2} = 6.5581 - 1.6988 \Delta G_{solv}$	R = 0.97359
Molecular electrostatic potential $V_{s,min}$	$q_{m_2} = 1.7966 - 0.33526 V_{s_{min}}$	R = 0.98695
Solubility S	$q_{m_2} = 7.4611 + 3.242 \log S$	R = 0.98994

simultaneously a HBA and a hydrogen bond donor (HBD): first, 1-butanol can be hydrogen bonded to hydrogen atom of water or hydroxyl molecules (as MEK and butyraldehyde); secondly, 1-butanol can be directly hydrogen bonded to the O atom of TiO_2. It may be the reason why 1-butanol has a higher q_{m1} value than MEK and butyraldhehyde. Other molecules (*n*-butane, pentane, isobutane, hexane) are neither HBA nor HBD and can only be bound due to less important London interactions to water and/or TiO_2.

For the maximum adsorption capacity on the second part of the isotherm curve q_{m2}, better correlations were obtained with molecular descriptors linked to the possible dissolution of species into water clusters at the catalyst surface. Table 4, below, displays the best obtained results.

It appears that the more the volatile compound is soluble in water, the higher is the sorption capacity q_{m2}, as it can be seen by the positive linear relation between q_{m2} and log S and by the negative linear relation between q_{m2} and log K_{ow}. In a similar manner, the molecular descriptors ΔG_{solv} and $V_{s,min}$ relate the affinity of the tested molecules with a hydrophilic medium like water. As already assumed in a previous paper, at a relative humidity of 50%, it can be considered that the whole surface of TiO_2 is covered with water clusters [23]. Consequently, the sorption of VOCs is mainly governed by absorption process.

3.2 Photocatalytic degradation

Photocatalytic degradations of the seven molecules were obtained at four different initial concentrations ranging from 9.75 to 36.4 mmol m^{-3}. Each experiment was repeated twice to ensure the reproducibility of the results.

From the kinetic curves, initial reaction rates r_0 were calculated using the methodology described previously and plotted versus the initial concentration C_0. The results are drawn in Figures 4 and 5.

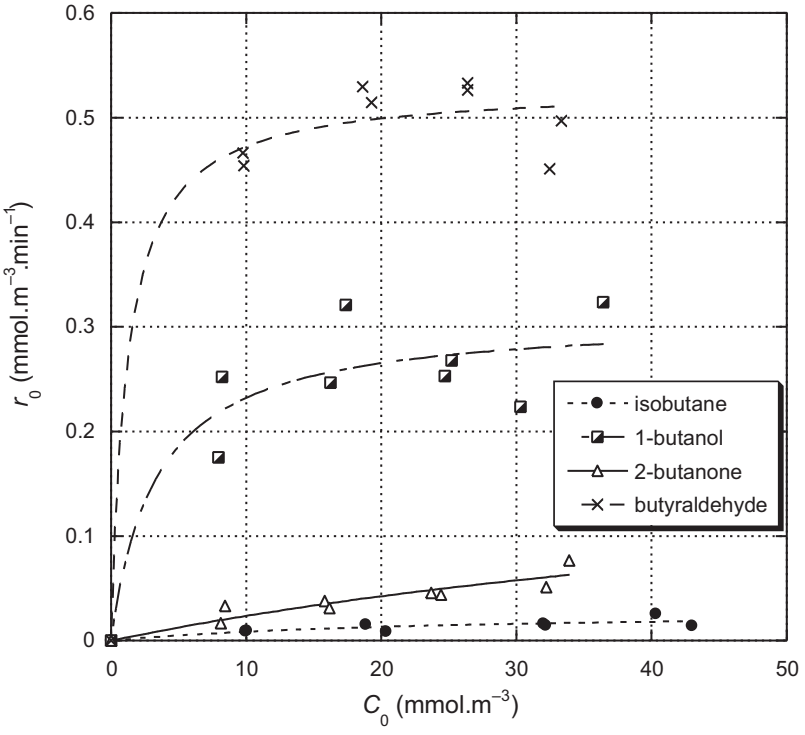

Figure 4 r_0 versus C_0 for 1-butanol, 2-butanone, butyraldehyde and isobutane.

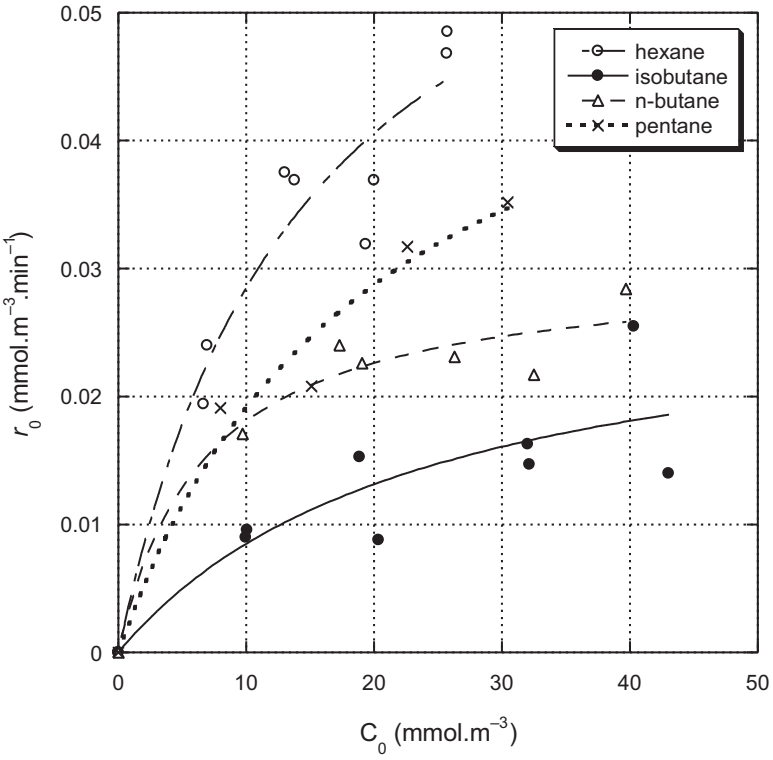

Figure 5 r_0 versus C_0 for hexane, pentane, n-butane and isobutane

As seen in Figures 4 and 5, initial degradation rates (r_0) increase at the beginning with the increase of VOCs concentration and seem to reach a plateau, especially for butyraldehyde and 1-butanol. A non-linear least squares regression function was used to fit the experimental results to the global reaction rate equation (10). The k_g and K_A constants were determined for the whole set of tested VOCs. These calculations are presented in Table 5.

Despite satisfactory correlation coefficients, the errors on the constants are relatively high. As some experimental points in the C_0 range 0–10 mmol m^{-3} are missing, the values of K_A are approximated and a notable error appears on their calculations. For most of the calculated values, the error is larger than 50%. However, for k_g the relative error is less notable. On average, the relative error on k_g is approximately 18%, not taking into account iso-butane for which the relative error on k_g reaches 43%. For further investigations, it was chosen to work on k_g values only. As for adsorption, the tested molecules can be divided into two groups (alkanes and the three other compounds). Regarding k_g values, the photoreactivity order for the seven VOCs is ranking in the following order: butyraldehyde > 1-butanol >> hexane = 2-butanone = pentane > *n*-butane = iso-butane. This is consistent with previous work performed by Obee and Hay [38] and Hodgson et al. [15].

The work hereafter consists of finding simple relationships between the global reaction rate constant k_g first with physico-chemical parameters and then with the molecular descriptors presented in the previous part.

Table 5 Global reaction rate constants k_g and equilibrium constants K_A.

	k_g (mmol m^{-3} min^{-1})	K_A (m^3 mmol^{-1})	r
Iso-butane	**0.029** ± 0.013	0.041 ± 0.038	0.852
***n*-Butane**	**0.030** ± 0.004	0.149 ± 0.075	0.976
Pentane	**0.058** ± 0.016	0.049 ± 0.027	0.984
2-Butanone	**0.063** ± 0.006	0.117 ± 0.031	0.928
Hexane	**0.071** ± 0.015	0.068 ± 0.030	0.962
1-Butanol	**0.309** ± 0.041	0.300 ± 0.238	0.919
Butyraldehyde	**0.529** ± 0.027	0.831 ± 0.645	0.986

3.3 Relations with VOCs-hydroxyl radical rate constant, Henry's law constant and molecular descriptors

Hydroxyl radicals (OH°) are generally considered as the primary oxidizer attacking the organic compounds in photocatalytic reactions [14]. Consequently, it can be assumed that the reaction constant k_g should be

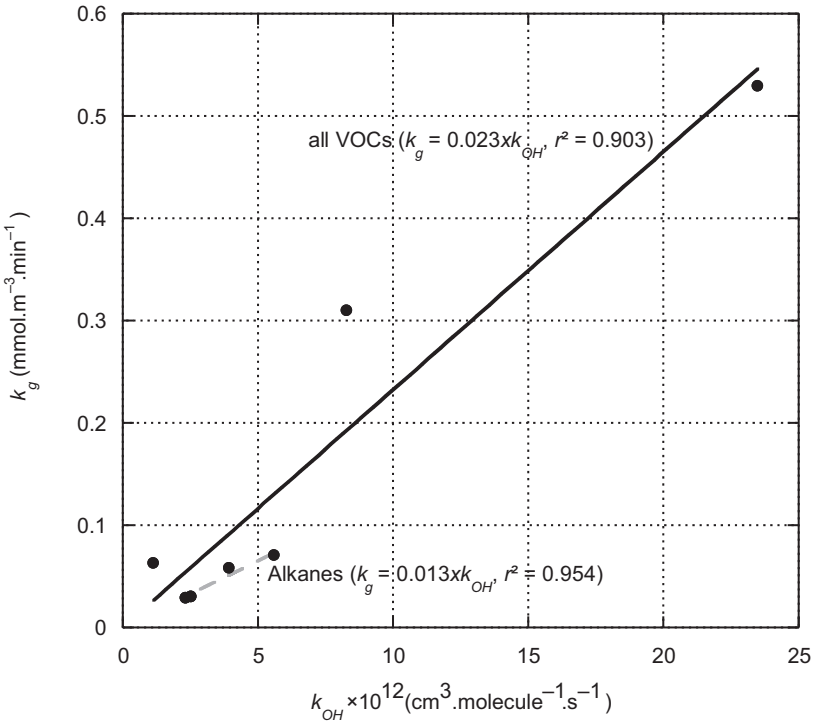

Figure 6 VOCs-OH° rate constant versus global reaction rate constant.

proportional to the VOCs-hydroxyl radical rate constant k_{OH}. In this work, a positive linear relation between k_g and k_{OH} with a determination coefficient of 0.903 was found (Figure 6). A similar result has been obtained by Yu et al. [14] but for aromatic hydrocarbons only. When the studied molecules are divided into two groups, one for the alkanes and one for the molecules with four atoms of carbon, the determination coefficients r^2 are better (0.9543 for alkanes and 0.9225 for C_4 molecules). The slope of the curves is lower for alkanes alone (0.0133). For molecules with four atoms of carbon, the slope has almost the same value than for the whole set of tested VOCs. The result indicates that the reactivity of a molecule has a great influence on the photocatalytic degradability of the molecule. However, as the determination coefficient is not high enough, it appears clearly that the k_{OH} parameter is not sufficient by itself to accurately determine the global reaction rate constant.

It has already been proved that water vapor plays a great role in adsorption and then in photocatalytic reaction. In the literature, few attempts of correlations between photocatalytic kinetic constants and Henry's law constant have been established; the work of Hodgson et al. [15] can be cited as an example.

Regressions between the global reaction rate constant k_g and the Henry's law constant were then performed in order to assess the possible influence of a water layer at the catalyst surface on the kinetic constant. Figure 7 below shows the obtained results.

A linear relation was found between k_g and $K°_H$ with a good r^2 coefficient (0.972) but in this case butyraldehyde was not taken into account. However, again, regarding Figure 7, it can be said that the only Henry's law constant is not sufficient to deduce the precise global reaction rate.

From the above results, it can be observed that none of the parameters taken into account alone is sufficient to correctly describe the behavior of the global reaction rate in function of the considered VOC. However, a combination of these parameters could permit to have access to a good prediction of the global reaction rate. A multiple linear regression (MLR) was performed between k_g, k_{OH} and $K°_H$. The obtained equation is

$$k_g = 0.0227.10^{12}k_{OH} + 0.0012K^{\circ}_H - 0.0248 \qquad [13]$$

The determination coefficient for this MLR reaches 0.988. In previous publications, Hodgson et al. [15] and Zorn et al. [39] found that photocatalytic reaction rate constants were also dependent on Henry's law constant ($K°_H$) and the gas-phase reaction rate constant with hydroxyl radicals (k_{OH}). However, the found relationships were not linear with the

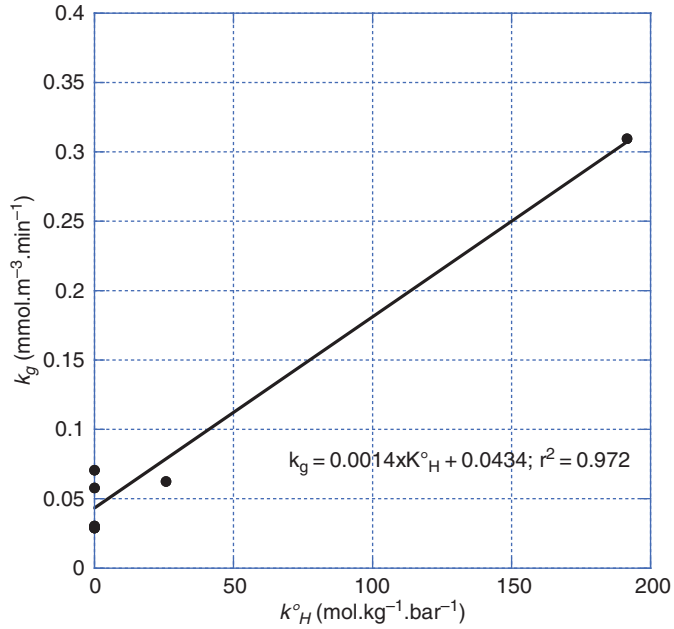

Figure 7 Henry's law constant versus global reaction rate constant.

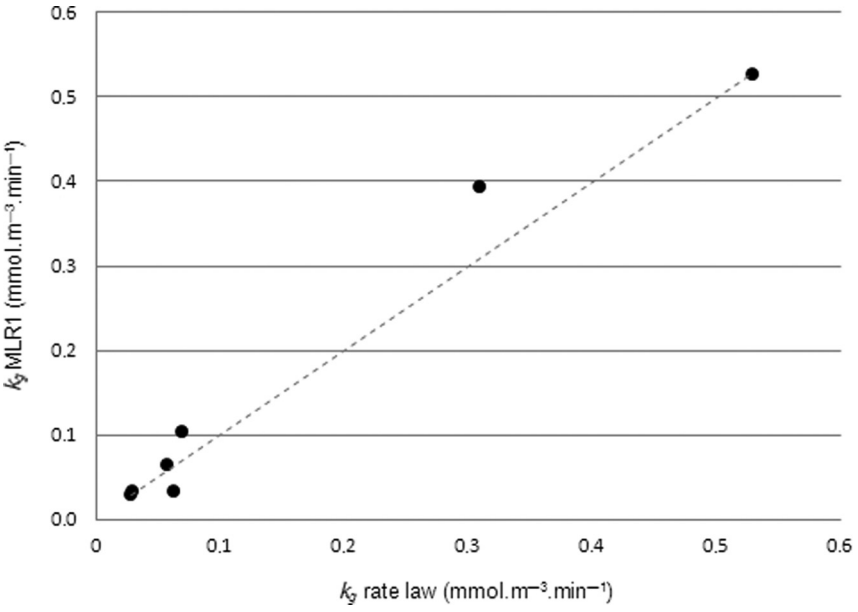

Figure 8 Results of the MLR for k_g as a function of k_{OH} and $K°_H$.

k_g, $K°_H$ and k_{OH} parameters but with the logarithms of these parameters. Figure 8 below displays the values of k_g calculated using this equation versus the values of k_g obtained by the rate law equation (Table 5).

To determine the weight of each of the physicochemical parameters k_{OH} and $K°_H$, reduced and centered variables were calculated and the MLRs were repeated, resulting in the following equation:

$$k_g{}^* = 0.9179 k_{OH}{}^* + 0.2930 K^\circ_H{}^* + 2.3232.10^{-18} \quad [14]$$

From the coefficients in this equation, it appears clearly that k_{OH} has a more predominant weight than $K°_H$. This means that the photocatalytic degradation is mainly governed by the reactivity of the molecule with hydroxyl radicals. However, the weight of $K°_H$ is not low enough to be neglected.

The first step of correlations was satisfactory, however, k_{OH} and $K°_H$ are not always available in the literature and cannot be always easily determined. The next step consists of finding relationships between the global reaction rate and molecular descriptors of the molecules. To do so, relations between k_{OH} and $K°_H$ parameters and molecular descriptors were searched.

From the correlation trials as a whole, it was possible to establish a relationship between k_{OH} and two molecular descriptors: hardness and E_{HOMO} (Figure 9).

For the whole set of tested molecules (except MEK), an exponential relation between k_{OH} and hardness was also valid ($k_{OH} = 0.75 \exp^{(-97.5\ hardness)}$, $r^2 = 0.973$). Similarly, an exponential relation was found between k_{OH} and E_{HOMO} ($k_{OH} = 7.93 \exp^{(63.08 E_{HOMO})}$, $r^2 = 0.970$) (Figure 10).

With the same objective, relationships were sought between $K°_H$ and molecular descriptors. For the Henry's law constant $K°_H$, exponential relationships were found with the solvation free energy ΔG_{solv} and the molecular electrostatic potential $V_{s,min}$. The equations are listed below:

$$K^\circ_H = 0.004 exp(-0.3059\, V_{s,min}),\ r^2 = 0.0981 \quad [15]$$

$$K^\circ_H = 0.0319 exp(-1.5845\, \Delta G_{solv}),\ r^2 = 0.998 \quad [16]$$

3.4 Global relation between kg and molecular descriptors

The global kinetic rate was described in a satisfactory way by k_{OH} and $K°_H$ in a MLR. The latter parameters were also well described by four molecular descriptors, the hardness and E_{LUMO} for K_{OH} and the solvation free energy and the molecular electrostatic potential for $K°_H$. From the above results, it was possible to find a global relationship between the kinetic constant k_g and the said molecular descriptors. For instance, the relationship with ΔG_{solv} and hardness would be as follows:

$$k_g = 0.017.10^{12} e^{(-97.5\ hardness)} + 3.828.10^{-5} e^{(-1.584\, \Delta G_{solv})} - 0.0248 \quad [17]$$

Also, the relationship including E_{HOMO} and ΔG_{solv} would be:

$$k_g = 1.8.10^{11} e^{(63.08 E_{HOMO})} + 3.828.10^{-5} e^{(-1.584\, \Delta G_{solv})} - 0.0248 \quad [18]$$

Figure 11 below displays the values of k_g calculated using eq. [17] versus the values of k_g obtained by the rate law equation (Table 5).

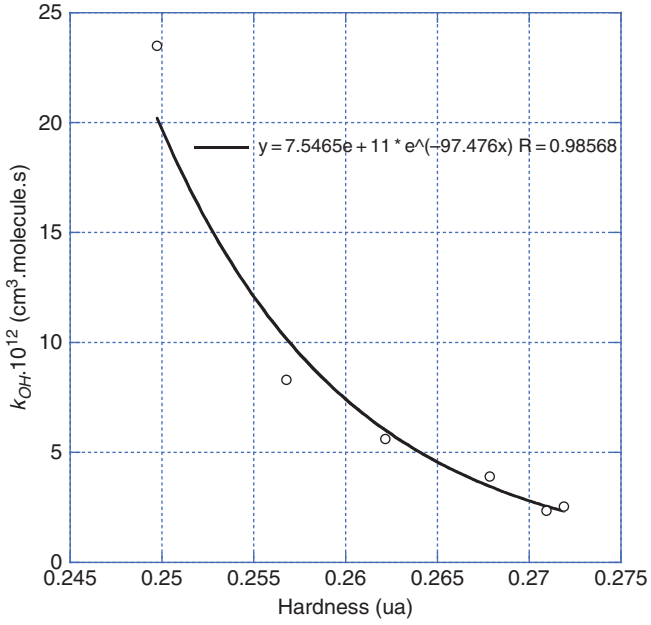

Figure 9 Exponential relation between k_{OH} and hardness for the set of molecules (without MEK).

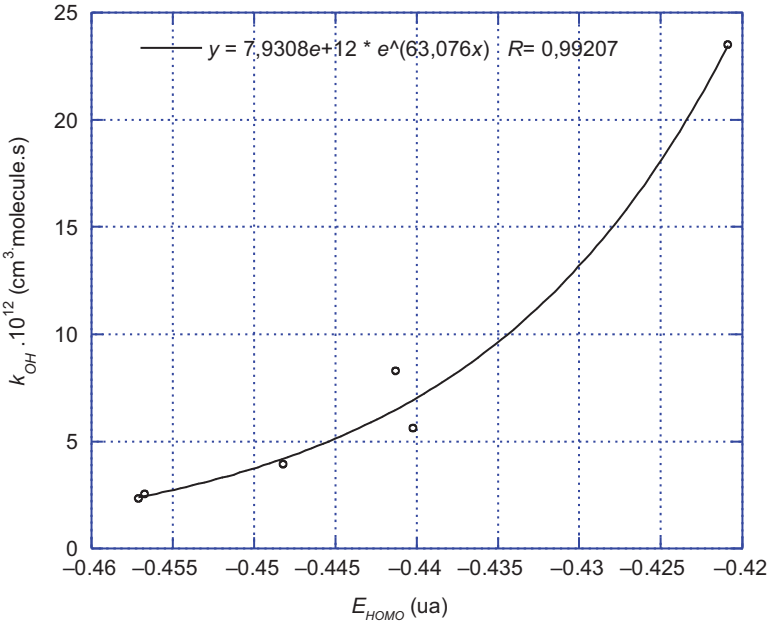

Figure 10 Exponential relation between k_{OH} and E_{LUMO} for the set of molecules (without MEK).

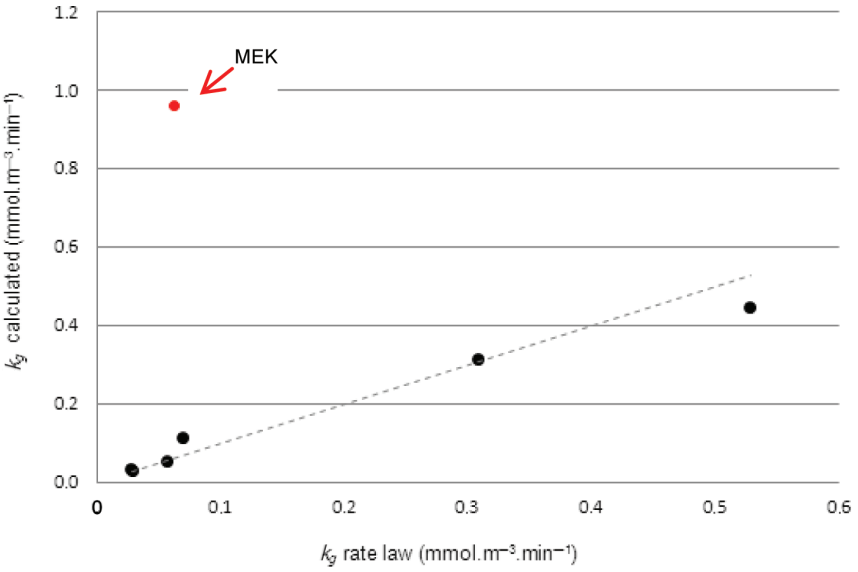

Figure 11 Results of the correlation for k_g as a function of hardness and solvation free energy.

3.5 MEK

The calculated values of k_g with eq. [17] are relatively close to values obtained by the rate law with the exception of MEK. These results showed that it is possible to correlate the obtained photocatalytic experimental constants to molecular descriptors of the tested molecules.

4 Conclusion

The photocatalytic oxidation of seven indoor VOCs was experimentally investigated using a nanocrystalline TiO_2-dip-coated catalyst. Physico-chemical properties like the solubility, the partition coefficient octanol–water, the Henry's constant and the VOC-hydroxyl radical rate constant were put into relation with the kinetic and

equilibrium constants obtained during the experimental phase. VOCs molecular descriptors have been calculated by molecular modeling. They are used to represent the van der Waals forces or the adsorption phenomenon, the affinity with hydrophilic surfaces or aqueous medium and finally the electronic stability of the molecules and their reactivity. Correlation between kinetic and equilibrium constants and the molecular descriptors were also assessed. The main objectives of this work were to establish simple relationships that will be useful to deepen the understanding of gas-phase heterogeneous photocatalytic mechanisms and for further prediction of degradation rates.

Two key results should be highlighted at this point. First, looking at the adsorption phenomenon of the tested molecules onto the mesoporous TiO_2-anatase catalyst, it was suggested that the molecules' adsorption is primarily governed by a chemical adsorption onto the surface rather than a physical adsorption in relation to the van der Waals forces. For high molecular concentration, it is clearly mentioned that a dissolution or absorption process occurs.

Second, looking at the main correlations found in relation to the kinetic constant of reaction, it is shown that the reaction rate can be governed not only by the reactivity of the molecules with OH° radical, but also the affinity of the molecule with hydrophilic surface. It can be suggested that the $K°_H$ constant, by extending the solvation free energy or the molecular electrostatic potential, may express the possible diffusion of the molecule in a water layer at the catalyst surface influencing the global kinetic rate.

This study has shown that QSAR can be a useful approach for the understanding of heterogeneous mechanisms.

References

1. Bernstein JA, Alexis N, Bacchus H, Bernstein IL, Fritz P, Horner E, et al. The health effects of nonindustrial indoor air pollution. J Allergy Clin Immunol 2008;121:585–91.
2. Salthammer T. Critical evaluation of approaches in setting indoor air quality guidelines and reference values. Chemosphere 2011;82:1507–17.
3. Pichat P, Disdier J, Hoang-Van C, Mas D, Goutailler G, Gaysse C. Purification/deodorization of indoor air and gaseous effluents by TiO_2 photocatalysis. Catal Today 2000;63:363–9.
4. Zhao J, Yang X. Photocatalytic oxidation for indoor air purification: a literature review. Building Environ 2003;38:645–54.
5. Kim SB, Hong SC. Kinetic study for photocatalytic degradation of volatile organic compounds in air using thin film TiO_2 photocatalyst. Appl Catal B: Environ 2002;35:305–15.
6. Raillard C, Héquet V, Le Cloirec P, Legrand J. TiO_2 coating type influencing the role of water on the photocatalytic oxidation of methyl ethyl ketone in the gas phase. Appl Catal B: Environ 2005;59:213–20.
7. Watanabe T, Nakajima A, Wang R, Minabe M, Koizumi S, Fujishima A, Hashimoto K. Photocatalytic activity and photoinduced hydrophilicity of titanium dioxide coated glass. Thin Solid Films 1999;351:260–3.
8. Fujishima A, Rao TN, Tryk DA. Titanium dioxide photocatalysis. J Photochem Photobiol C: Photochem Rev 2000;1:1–21.
9. Kemmitt T, Al-Salim NI, Waterland M, Kennedy VJ, Markwitz A. Photocatalytic titania coatings. Curr Appl Phys 2004;4:189–92.
10. Nuida T, Kanai N, Hashimoto K, Watanabe T, Ohsaki H. Enhancement of photocatalytic activity using UV light trapping effect. Vacuum 2004;74:729–33.
11. Guan K. Relationship between photocatalytic activity, hydrophilicity and self-cleaning effect of TiO_2/SiO_2 films. Surf Coat Technol 2005;191:155–60.
12. Pichat P. Some views about indoor air photocatalytic treatment using TiO_2: conceptualization of humidity effects, active oxygen species, problem of C_1–C_3 carbonyl pollutants. Appl Catal B: Environ 2010;99:428–34.
13. Raillard C, Héquet V, Le Cloirec P. Influence of aqueous solubility of various VOCs on their photocatalytic degradation. J Adv Oxid Technol 2007;10:101–6.
14. Yu K-P, Lee GW, Huang W-M, Wu C, Yang S. The correlation between photocatalytic oxidation performance and chemical/physical properties of indoor volatile organic compounds. Atmos Environ 2006;40:375–85.
15. Hodgson AT, Destaillats H, Sullivan DP, Fisk WJ. Performance of ultraviolet photocatalytic oxidation for indoor air cleaning applications. Indoor Air 2007;17:305–16.
16. D'Oliveira J-C, Minero C, Pelizetti E, Pichat P. Photodegradation of dichlorophenols and trichlorophenols in TiO_2 aqueous suspensions: kinetic effects of the positions of the Cl atoms and identification of the intermediates. J Photochem Photobiol A: Chem 1993;72:261–7.
17. Amalric L, Guillard C, Blanc-Brude E, Pichat P. Correlation between the photocatalytic degradability over TiO_2 in water of meta and para substituted methoxybenzenes and their electron density, hydrophobicity and polarisability properties. Water Res 1996;30:1137–42.
18. San N, Hatipoğlu A, Koçtürk G, Çinar Z. Photocatalytic degradation of 4-nitrophenol in aqueous TiO_2 suspensions: theoretical prediction of the intermediates. J Photochem Photobiol A: Chem 2002;146:189–97.
19. Parra S, Olivero J, Pulgarin C. Relationships between physicochemical properties and photoreactivity of four biorecalcitrant phenylurea herbicides in aqueous TiO_2 suspension. Appl Catal B: Environ 2002;36:75–85.

20. Fogler HS. Eds. Elements of chemical reaction engineering, 2nd ed. Prentice-Hall PTR: Upper Saddle River, 1992.
21. Choi H, Stathatos E, Dionysiou DD. Synthesis of nanocrystalline photocatalytic TiO_2 thin films and particles using sol-gel method modified with non-ionic surfactants. Thin Solid Films 2006;510:107–14.
22. Raillard C, Héquet V, Le Cloirec P, Legrand J. Kinetic study of ketones photocatalytic oxidation in gas phase using TiO_2-containing paper: effect of water vapor. J Photochem Photobiol A: Chem 2004;163:425–31.
23. Maudhuit A, Raillard C, Héquet V, Le Coq L, Sablayrolles J, Molins L. Adsorption phenomena in photocatalytic reactions: the case of toluene, acetone and heptane. Chem Eng J 2011;170:464–70.
24. Sauer ML, Ollis DF. Acetone oxidation in a photocatalytic monolith reactor. J Catal 1994;149:81–91.
25. Frisch MJ, et al. Gaussian 03 rev. E01. Wallingford, CT: Gaussian, Inc., 2004.
26. Le Guennec M, Evain K, Illien B. Calculation of static mean polarisability and polarisability anisotropy. Statistical comparison with the results of gases and influence of the geometrical parameters. J Mol Struct (Theochem) 2001;542:167–76.
27. Pearson RG. Absolute electronegativity and absolute hardness of Lewis acids and bases. J Am Chem Soc 1985;107:6801–6.
28. Wong MW, Wiberg KB, Frisch MJ. Ab initio calculation of molar volumes: comparison with experiment and use in solvation models. J Comput Chem 1995;16:385–394.
29. Jensen F. Introduction to computational chemistry. Chichester, England: Wiley, 2007.
30. Yalkowski SH, He Y. Handbook of aqueous solubility data. Boca Raton, Florida, United States of America: CRC Press, 2003.
31. Atkinson R. Gas-phase tropospheric chemistry of organic compounds: a review. Atmos Environ 2007;41:200–40.
32. Staudinger J, Roberts PV. A critical compilation of Henry's law constant temperature dependence relations for organic compounds in dilute aqueous solutions. Chemosphere 2001;44:561–76.
33. Yaws CL, Yang H-C. Henry's law constant for compound in water. In: Yaws CL, editor. Thermodynamic and physical property data. Houston, TX: Gulf Publishing Company, 1992:181–206.
34. Boulamanti AK, Philippopoulos CJ. Photocatalytic degradation of C5-C7 alkanes in the gas-phase. Atmos Environ 2009;43:3168–74.
35. Joung S-K, Amemiya T, Murabayashi M, Cai R, Itoh K. Chemical adsorption of phosgene on TiO_2 and its effect on the photocatalytic oxidation of trichloroethylene. Surf Sci 2005;598:174–84.
36. Thanikaivelan P, Subramanian V, Raghava Rao J, Nair BU. Application of quantum chemical descriptor in quantitative structure activity and structure property relationship. Chem Phys Lett 2000;323:59–70.
37. Obee TN, Brown RT. TiO_2 photocatalysis for indoor air applications: effects of humidity and trace contaminant levels on the oxidation rates of formaldehyde, toluene and 1,3-butadiene. Environ Sci Technol 1995;29:1223–31.
38. Obee TN, Hay SO. The estimation of photocatalytic rate constants based on molecular structure: extending to multi-component systems. J Adv Oxid Technol 1999; 4:147–52.
39. Zorn ME, Hay SO, Anderson MA. Effect of molecular functionality on the photocatalytic oxidation of gas-phase mixtures. Appl Catal B: Environ 2010;99:420–7.